HHS Public Access

Author manuscript

Cell. Author manuscript; available in PMC 2015 July 06.

Published in final edited form as:

Cell. 2012 July 20; 150(2): 351–365. doi:10.1016/j.cell.2012.05.041.

Noncanonical Wnt Signaling Maintains Hematopoietic Stem Cells in the Niche

Ryohichi Sugimura[1], **Xi C. He**[1], **Aparna Venkatraman**[1,2], **Fumio Arai**[3], **Andrew Box**[1], **Craig Semerad**[1], **Jeffrey S. Haug**[1], **Lai Peng**[4], **Xiao-bo Zhong**[4], **Toshio Suda**[3], and **Linheng Li**[1,5,*]

[1]Stowers Institute for Medical Research, 1000 East 50th Street, Kansas City, MO 64110, USA

[2]Centre for Stem Cell Research, Christian Medical College, Vellore 632002, India

[3]Department of Cell Differentiation, School of Medicine, Keio University, 35 Shinano-machi, Shinjuku-ku, Tokyo 160-8582, Japan

[4]Department of Pharmacology, Toxicology, and Therapeutics, The University of Kansas Medical Center, 3901 Rainbow Boulevard, Kansas City, KS 66160, USA

[5]Department of Pathology and Laboratory Medicine, The University of Kansas Medical Center, 3901 Rainbow Boulevard, Kansas City, KS 66160, USA

SUMMARY

Wnt signaling is involved in self-renewal and maintenance of hematopoietic stem cells (HSCs); however, the particular role of noncanonical Wnt signaling in regulating HSCs in vivo is largely unknown. Here, we show Flamingo (Fmi) and Frizzled (Fz) 8, members of noncanonical Wnt signaling, both express in and functionally maintain quiescent long-term HSCs. Fmi regulates Fz8 distribution at the interface between HSCs and N-cadherin$^+$ osteoblasts (N-cad$^+$OBs that enrich osteoprogenitors) in the niche. We further found that N-cad$^+$OBs predominantly express noncanonical Wnt ligands and inhibitors of canonical Wnt signaling under homeostasis. Under stress, noncanonical Wnt signaling is attenuated and canonical Wnt signaling is enhanced in activation of HSCs. Mechanistically, noncanonical Wnt signaling mediated by Fz8 suppresses the Ca^{2+}-NFAT- IFNγ pathway, directly or indirectly through the CDC42-CK1α complex and also antagonizes canonical Wnt signaling in HSCs. Taken together, our findings demonstrate that noncanonical Wnt signaling maintains quiescent long-term HSCs through Fmi and Fz8 interaction in the niche.

INTRODUCTION

Wnt signaling has been well studied for its role in regulating hematopoietic stem cells (HSCs) (Reya and Clevers, 2005). Wnt signaling can be subdivided into canonical and noncanonical pathways.

*Correspondence: lil@stowers.org.

SUPPLEMENTAL INFORMATION

Supplemental Information includes Extended Experimental Procedures, and seven figures, and three tables and can be found with this article online at http://dx.doi.org/10.1016/j.cell.2012.05.041.

Canonical Wnt signaling in regulating stem cell self-renewal in hair follicle and intestine has been well documented (Blanpain and Fuchs, 2009; Radtke and Clevers, 2005). However, its role in regulating hematopoietic stem cell self-renewal and maintenance is controversial (Malhotra and Kincade, 2009).

Noncanonical Wnt signaling regulates cellular polarization, controls nuclear localization of nuclear factor of activated T cell (NFAT) transcriptional factor via either calcium (Ca^{2+}) or CK1α, and suppresses canonical Wnt signaling (Mikels and Nusse, 2006; Moon et al., 1993; Murphy and Hughes, 2002). Different noncanonical Wnts may have different effects in this regard. For example, Wnt5a exerts dual functions: stimulating Ca^{2+}-induced NFAT nuclear localization or restricting NFAT nuclear localization via Cdc42-CK1α complex (Dejmek et al., 2006; Huang et al., 2011; Saneyoshi et al., 2002). However, Wnt11 inhibits Ca^{2+} influx through restricting L-type calcium channel (LTCC) (Panáková et al., 2010). These observations suggest that noncanonical Wnts exert tissue-, stage-, and frizzled (Fz)-dependent functions with regard to regulation of Ca^{2+} level and NFAT nuclear translocation. Wnt5a maintains HSCs in vitro culture and augments repopulation efficiency of human HSCs transplanted into mice (Murdoch et al., 2003; Nemeth et al., 2007). However, the role and the underlying mechanism of non-canonical Wnt signaling in HSC regulation in vivo are largely unknown.

We previously reported that *Flamingo* (*Fmi/Celsr2*) (Usui et al., 1999) and *Fz8* (Gregory et al., 2010) are predominantly expressed in primitive HSCs (Akashi et al., 2003). Fmi is a type of cadherin adhesion molecule that also has a G-protein-coupled-receptor (GPCR) domain, which facilitates Fz-mediated noncanonical Wnt signaling (Halbleib and Nelson, 2006). Functionally, Fmi is known to cooperate with Fz to regulate neuronal growth and keratinocytes during development through contact inhibition (Devenport and Fuchs, 2008; Zhou et al., 2008). Whether Fmi and Fz8 play a role in regulating HSCs is yet to be determined.

For long-term maintenance of adult stem cells, a subset of stem cells needs to be kept in long-term quiescence in a specialized niche (Arai et al., 2004; Haug et al., 2008; Wilson et al., 2008; Zhang et al., 2003). Quiescent long-term HSCs (LT-HSCs) are mainly located in the endosteum of the trabecular bone region (TBR), where HSCs are directly attached to N-cadherin^{+} osteoblasts (N-cad^{+}OBs) known to enrich osteoprogenitors (Wilson et al., 2008; Xie et al., 2009; Zhang et al., 2003). In addition to BMP signaling, other key signals emanating from this niche component to maintain HSC quiescence remain largely unknown (Li and Clevers, 2010).

In this work, we demonstrate that noncanonical Wnt signaling mediated by Fmi and Fz8 plays a critical role in the long-term maintenance of quiescent HSCs by suppressing the Ca^{2+}-NFAT-interferon-gamma (IFNγ) pathway and antagonizing canonical Wnt signaling.

RESULTS

Fmi Regulates Noncanonical Wnt Receptor Fz8 Distribution in Quiescent LT-HSCs

We previously reported expression of both *Fmi* and *Fz8* in quiescent HSCs (Rhodamine^{lo} or $Rh_{123}{}^{lo}$LSK) (Akashi et al., 2003). To further confirm *Fmi* expression in HSCs, we compared its expression levels in LT-HSCs (CD34^{-}Flk2^{-}LSK), short-term (ST)-HSCs (CD34^{+}Flk2^{-}LSK), and multipotent progenitors (MPPs) (CD34^{+}Flk2^{+}LSK) (Figures 1A and 1B) (Yang et al., 2005). *Fmi* mRNA level was 2-fold and 3-fold higher in LT-HSCs compared to ST-HSCs and MPPs, respectively (Figure 1C).

We next examined *Fmi* and *Fzs* expression in quiescent LT-HSCs identified by Scl-tTA-induced H2B-GFP label-retaining cells (LRCs) (H2B-GFP hereinafter) (Tumbar et al., 2004; Wilson et al., 2008) (Figure 1D). We excluded H2B-GFP background signal derived from non-tTA-induced animals (Challen and Good-ell, 2008; Wilson et al., 2008) and set H2B-GFP gate at the high position (H2B-GFP^{hi}) (Figures S1A and S1B available online). We confirmed that H2B-GFP^{hi}LSK enriched LT-HSCs 5-fold and reduced MPPs 4.8-fold compared to H2B-GFP^{-}LSK (Figure 1E). We sorted Flk2^{-}LSK HSCs (to exclude MPPs) into H2B-GFP^{-} (active) and H2B-GFP^{hi} (quiescent) subpopulations (Figure 1F). Consistent with a previous report (Wilson et al., 2008), we found that *CD34* mRNA was expressed at a much higher level in active HSCs than in quiescent HSCs (Figure 1G). *Fmi* expression was 12.5-fold higher in quiescent HSCs than in active HSCs (Figure 1H). Among Fzs, noncanonical Wnt receptor *Fz8* was the one that showed significantly higher (3-fold) expression in quiescent HSCs than in active HSCs (Figure 1I and Figure S1C).

Fmi and Fz8 proteins were expressed in LT-HSCs (Figure 1J). Expression of both Fmi and Fz8 was detected in 18% of H2B-GFP^{-} HSCs compared to 70% of H2B-GFP^{hi} HSCs (Figures 1K and 1L). We also detected the expression of Fmi and Fz8 in CD150^{+}CD34^{-}Flk2^{-}LSK HSCs (Figure S1D). We used a hypoxic-related HSC marker GRP78 (Miharada et al., 2011) and detected Fmi and Fz8 expression in GRP78^{+}CD34^{-}LSK HSCs as well (Figure S1E).

We next examined whether Fmi determines the cellular distribution of Fz protein. Through overexpressing Fmi and Fz8 fused with fluorescent proteins in 293T cells, we found that Fz8 distributed randomly when Fmi was not expressed; however, Fz8 was restricted to the site where Fmi was present (Figure S2A). To ascertain whether Fmi determined Fz8 distribution in HSCs, we used an in vitro culture system of HSCs with OP9, an osteoprogenitor cell line (Mahmood et al., 2011; Nakano et al., 1994). (Figure S2B). Fmi was present at the interface between sorted HSC (labeled with GFP) and OP9 cells (Figure 1M). When Fmi was knocked down, the distribution of Fz8 protein became random (Figures 1N and 1O; Figure S2C). In addition, lack of Fmi in OP9 resulted in random distribution of Fz8 in LSK cells (Figures 1P and 1Q; Figure S2E), suggesting that homophilic interaction between two Fmi located in adjacent HSC and OP cells functions to restrict Fz8 at the HSC-OP9 interface. In contrast, knockdown of Fz8 did not affect Fmi protein distribution (Figure S2D). These results show that Fmi and Fz8 are both expressed in quiescent LT-HSCs and that Fmi restricts Fz8 distribution at the interface between HSCs and osteoprogenitors in vitro.

Fmi and Fz8 Colocalize Predominantly at the Interface between Quiescent LT-HSCs and N-cad^{+}OBs in TBR

We next confirmed our in vitro observation of the Fmi and Fz8 co-localization in vivo. Because HSCs tend to home to trabecular bone region (TBR) (Figures 2A and 2B) rather than compact bone region (CBR) (Xie et al., 2009), we examined the in vivo distribution of LT-HSCs expressing both Fmi and Fz8 in different bone regions (Figure 2B). We detected a majority (67%) of these LT-HSCs derived from TBR, but only 31% of LT-HSCs derived from CBR (Figures 2C–2E).

We next determined the distribution of quiescent LT-HSCs in the sagittal section of the femur. We identified quiescent LT-HSCs using the H2B-GFP^{hi}LRCs, and we compared the distribution of quiescent LT-HSCs between TBR and CBR (Figures 2F–2H). Flow cytometry analysis showed that the frequency of quiescent HSCs (H2B-GFP^{hi} LRCs) was more than 3-fold higher in TBR than in CBR (Figure 2F). Immunostaining confirmed this observation and revealed that H2B-GFP LRCs were mainly detected in the TBR compared to the CBR (Figures 2G and 2H).

We then examined the correlation between the distribution of quiescent LT-HSCs (H2B-GFP^{hi}LRCs) and the distribution of niche components known to regulate HSCs, including endothelial cells, Nestin^{+} MSCs, and N-cad^{+}OBs (Kiel et al., 2005; Méndez-Ferrer et al., 2010; Wilson et al., 2008; Xie et al., 2009; Zhang et al., 2003). Using a CD31-GFP endothelial reporter (established in our lab) and Nestin-GFP reporter (Mignone et al., 2004), we found that CD31-GFP^{+} endothelial cells and Nestin-GFP^{+} cells were distributed in both TBR and CBR without bias (Figures 2I–2L). In contrast, N-cad^{+}OBs were predominantly detected in TBR but rarely in CBR (Figures 2M and 2N). The specificity of a newly generated anti-N-cad monoclonal antibody was confirmed by loss of N-cad staining in the N-cad knockout mice (Figures 2O and S3A). We detected expression of Fmi and Fz8 in N-cad^{+}OBs mainly in the TBR endosteum (yellow arrow; compare Figures 2M and 2P to Figures 2N and 2Q).

Next, we compared the relationship between Fmi and other niche markers (Figures 2R–2W). We found that Fmi expression was almost absent in CD31-GFP^{+} endothelial cells (Figure 2R), low in Nestin-GFP^{+} cells (Figure 2S), and high in N-cad^{+}OBs (Figure 2T). Fz8 was also expressed in N-cad^{+}OBs (Figure 2U). Notably, we detected Fmi or Fz8 at the interface between H2B-GFP^{hi}LRCs and N-cad^{+}OBs in the TBR endosteum (Figures 2U and 2V). The colocalization of Fmi and Fz8 was observed in H2B-GFP^{hi} LRC attached to the surface of TB (Figure S2F).

To identify which subset of osteoblasts (OBs) interacts with H2B-GFP^{hi} LRC, we first examined OP9 osteoprogenitor cells and observed the colocalization of Fmi and Fz8 at the interface between sorted H2B-GFP^{hi} Flk2^{-}LSK and OP9 (Figure 2X; Movie S1), as well as sorted LT-HSCs and OP9 (Figure S2G). This co-localization was observed neither in adjacent H2B-GFP^{-} Flk2^{-}LSK (Figure 2X) nor in ST-HSCs (Figure S2G). To confirm this in vivo, we performed immunoassay on consecutive sections and revealed a colocalization of Fmi and Fz8 at the interface between H2B-GFP^{hi} LRC and N-cad^{+}OB (Figure S3B). We further verified this colocalization with four-color immunostaining and three-dimensional

(3D) high-resolution imaging (Figure 2Y; Movie S2). In summary, quiescent LT-HSCs are found more in TBR than in CBR. Fmi and Fz8 are colocalized at the interface between quiescent LT-HSCs and N-cad$^+$OBs.

N-cad$^+$OBs Maintain a Dominant Noncanonical Wnt Signaling, which Is Attenuated under Stress

We used RNA-sequencing analysis to examine the expression patterns of ligands and inhibitors for canonical and noncanonical Wnt signaling in the niche components, including CD31$^+$VEGFR2$^+$ cells (endothelial progenitor cells), Nestin-GFP$^+$ MSC-like cells, N-cad$^+$OBs, and Col2.3-GFP$^+$ mature OBs (Kalajzic et al., 2002; Lyden et al., 2001; Méndez-Ferrer et al., 2010; Xie et al., 2009; Zhang et al., 2003) (Figure 3A). Expression level was measured by fragments per kilobase of exon per million fragments mapped (FPKM) (Trapnell et al., 2010). Expression of canonical Wnt ligands overall was either absent or low (3–6 FPKM) in all three niche components (Figure 3B; Table S1). In contrast, expression of canonical Wnt inhibitors was much higher (15–168 FPKM) and mainly in Nestin-GFP$^+$ cells, N-cad$^+$OBs, and mature OBs, with N-cad$^+$OBs expressing the highest levels (Figure 3C). Noncanonical Wnt ligands overall were expressed at comparable levels in Nestin-GFP$^+$ cells, mature OBs, and N-cad$^+$OBs, except for *Wnt6* and *Wnt16*, which were predominantly expressed in N-cad$^+$OBs (Figure 3D). CD31$^+$VEGEFR2$^+$ endothelial cells expressed low-level *Wnt5b* (Figure 3D), but Wif1, a noncanonical Wnt inhibitor, was expressed at highest level in Nestin-GFP$^+$ cells among these stromal cells. These observations suggest that the N-cad$^+$OB niche provides a microenvironment in which canonical Wnt signaling is suppressed and noncanonical Wnt signaling is predominant in homeostasis.

In response to stress, expansion of N-cad$^+$OBs precedes the activation and subsequent expansion of HSCs (Dominici et al., 2009) (Figures 3E–3I). The correlation between an increase in N-cad$^+$OBs and activation of HSCs (Dominici et al., 2009) suggested that 5FU stress could also induce dynamic changes in the expression of Wnt ligands in N-cad$^+$OBs. We found that expression of noncanonical ligands *Wnt11* and *Wnt16*, as well as canonical Wnt inhibitors *Dkk1* and *Sfrp4*, was diminished (Figures 3J and 3K; Figure S4). However, expression of canonical *Wnt7b* increased 6-fold post-5FU treatment (Figure 3L). These observations show that 5FU treatment decreases noncanonical Wnt signals but increases canonical Wnt signaling.

Next, we investigated the impact of 5FU on Fmi and Fz8 in HSCs. Using high-resolution 3D imaging to measure to what extent Fmi and Fz8 still colocalized post-5FU (Figure S3C), we found an ~8-fold decline of Fmi-Fz8 colocalization in LT-HSCs from TBR and a 2-fold decline from CBR (Figures 3M and 3N; S3D). This was due partially to the reduction of both Fmi and Fz8 mRNA in LT-HSCs post-5FU (Figures 3O–3P and S3E–S3G). The data indicate that, in addition to ligands in the niche, Fmi and Fz8 are also reduced in LT-HSCs post-5FU treatment.

We further asked whether 5FU induced a reduction of noncanonical Wnt signaling and a subsequent upregulation of canonical Wnt signaling in LT-HSCs (Figure 3Q). As Ca^{2+} is a major mediator of noncanonical Wnt signaling, we measured intracellular Ca^{2+} level by Fluo-3 (Minta et al., 1989). LT-HSCs post-5FU treatment showed a 2.5-fold increase of

intracellular Ca^{2+} level (Figure 3R) and an 8-fold increase of NFAT nuclear translocation (Figure 3S). The downstream target genes of NFAT, *IFN*γ and *Cox2*, were upregulated 6- and 2-fold, respectively, in LT-HSCs post-5FU treatment (Figure 3T). We also examined *IFN*γ expression in cytotoxic T cells and regulatory T cells (Treg, $CD4^+CD25^+$), and the latter is an HSC niche component as reported recently (Fujisaki et al., 2011). Notably, *IFN*γ expression was upregulated in Treg cells but not in cytotoxic T cells (Figure S3H).

To measure canonical Wnt signaling in LT-HSCs post-5FU treatment, we immunostained the sorted LT-HSCs with β-cat-pS552, which was phosphorylated by pAkt and became an active form in nucleus (He et al., 2007). pAkt staining was observed in more than 70% of LT-HSCs post-5FU treatment and in 10% of control LT-HSCs (Figure S3I). β-catenin-pS552 was detected in more than 50% of LT-HSCs post-5FU treatment and in 20% of control LT-HSCs (Figure 3U). This observation was confirmed by TOP-Gal staining (Figure 3V) and canonical Wnt target gene *Axin2* (Luis et al., 2011) (Figure 3W). The data indicate that 5FU induces a decline of noncanonical Wnt signaling and an increase of canonical Wnt signaling in LT-HSCs.

Fmi and Fz8 Maintain Quiescent LT-HSCs In Vivo

Because Fmi-Fz8 colocalization is enriched in quiescent HSCs and in the niche that expresses noncanonical Wnt ligands, we hypothesized that Fmi and Fz8 may have a role in maintaining HSC quiescence. Our preliminary results of knockdown of Fmi revealed a decrease in LT-HSCs but an increase in ST-HSCs and MPPs and functionally resulted in more than 50%–60% reduction of engraftment in repopulation assay (Figure S5A). To confirm this, we examined Fmi and Fz8 conventional knockout mouse models and found declines in the frequency (60% and 40%) and absolute number (80% and 50%) of LT-HSCs, respectively. The numbers of ST-HSCs and MPPs reduced as well in the $Fmi^{-/-}$ and $Fz8^{-/-}$ mice (Figures 4A and 4B). These results indicate functional requirements for Fmi- and Fz8-mediated noncanonical Wnt in maintaining LT-HSCs.

We used a hypoxic-related HSC marker GRP78 to stain LT-HSCs and observed a decline of $GRP78^+$ population from 31.3 ± 0.3% (control) to 11.8 ± 1.1% ($Fmi^{-/-}$) (Figures S5B and S5C), and an increase of mitochondrial activity in $Fmi^{-/-}$ LT-HSCs (Figure S5D). This suggested an increase in HSC activity when Fmi was lost. We therefore performed a cell cycle analysis and found that, within $Flk2^-$LSK HSCs, the percentage of quiescent (G0) cells declined from 23 ± 0.71% (control) to 15 ± 1.1% in $Fmi^{-/-}$, and from 22 ± 2.9% (control) to 16 ± 1.9% in $Fz8^{-/-}$ mice (Figures 4A, 4B, S5E, and S6A).

Next, we transplanted equal numbers (100) of LSK enriched with HSPCs (CD45.2) with rescue 2×10^5 bone marrow (BM) cells (CD45.1) into lethally irradiated recipient mice (CD45.1). We confirmed first that knockout of Fmi and Fz8 did not affect HSPC homing to BM and spleen (Figures S5F and S6B). After 16 weeks, hematopoietic reconstitution from donor-derived HSCs was reduced 80% by Fmi knockout (Figure 4C) and 70% by Fz8 knockout (Figure 4D). The analyses of recipients showed an 80% decrease of donor-derived LT-HSCs and a 70% decrease of donor-derived ST-HSCs in frequency and number (Figures 4E and 4F). In addition, knockout of either Fmi or Fz8 did not affect apoptosis (Figures S5G and S6C).

We next asked whether H2B-GFP^{hi} LRCs (quiescent HSCs) were affected by Fmi and Fz8 knockout. H2B-GFP^{hi} LRCs were predominantly observed in TBR in *Wt*, but less so in *Fmi*$^{-/-}$ (Figures 5A–5D) and *Fz8*$^{-/-}$ (Figures 5E–5H). Fz8 protein localization was observed at the interface between H2B-GFP^{hi} LRC and N-cad^{+}OB in *Wt* (Figure 5I); however, its distribution became random in remaining *Fmi*$^{-/-}$ H2B-GFP^{hi} LRCs (Figure 5J). The localization of Fmi protein was not affected in *Fz8*$^{-/-}$ LRC (Figures 5K and 5L), further supporting that the function of Fmi is to determine Fz8 distribution, but not vice versa. We then used flow assay to measure the population of H2B-GFP^{+} HSCs. The H2B-GFP signal intensity was significantly reduced in *Fmi*$^{-/-}$ and *Fz8*$^{-/-}$ LT-HSCs, suggesting that label retention was lost because of the decrease of quiescence in HSCs (Figures 5M and 5N). The frequency of H2B-GFP^{hi} LRCs in *Fmi*$^{-/-}$ and *Fz8*$^{-/-}$ decreased 8-fold in TBR and 10-fold in CBR (Figures 5O and 5P). Within TBR in *Wt*, 65% of H2B-GFP^{hi} LRCs were in direct contact with N-cad^{+}OBs, compared to 20% in *Fmi*$^{-/-}$ and 10% in *Fz8*$^{-/-}$ mice, respectively (Figures 5Q and 5R). Taken together, these observations provide additional evidence to support the conclusion that Fmi and Fz8 facilitate the maintenance of quiescent LT-HSCs in vivo.

Fz8 Maintains Quiescent HSCs by Suppressing NFAT-Induced IFNγ Expression and Antagonizing Canonical Wnt Signaling

We then investigated the underlying molecular mechanism by which Fmi and Fz8-mediated noncanonical Wnt signaling maintains quiescent LT-HSCs (Figure 6A). Our RNA sequencing of LT-HSCs showed a much higher expression level of *Cacnb1*, encoding the β1 subunit of LTCC, compared to other voltage-dependent Ca^{2+} channels (Table S2). Using immunoassay, we found Fz8 colocalized with LTCC in H2B-GFP^{hi} cells but not in adjacent H2B-GFP^{-} cells (Figure 6B). We further confirmed this by detecting colocalization of Fz8 and LTCC in H2B-GFP^{hi} HSCs but not in H2B-GFP^{-} HSCs. In the active HSCs, the LTCC distribution was randomly distributed (Figure 5C). This colocalization was disturbed in *Fz8*$^{-/-}$ H2B-GFP^{hi} LRC (Figure S7A). We observed a 2-fold increase of Ca^{2+} in the *Fz8*$^{-/-}$ LT-HSCs (Figures 6D, S7B, and S7C). Furthermore, while addition of Wnt11 had only a slight effect, Wnt5a reduced Ca^{2+} level in LT-HSCs by 30%. In addition, the increased Ca^{2+} level by Fz8 knockout could not be rescued by Wnt5a (Figure S7D). These data show that noncanonical Wnt signaling mediated by Fz8 controls the intracellular Ca^{2+}level via LTCC in HSCs, coinciding with the quiescent versus active state of HSCs.

We next asked whether Cdc42-Pak1-CK1α complex is involved in regulation of NFAT nuclear localization. CK1α was colocalized with NFAT in cytoplasm of *Wt* H2B-GFP^{hi} LRC. In contrast, NFAT was localized in the nucleus of *Fz8*$^{-/-}$ H2B-GFP^{hi} LRC (Figure 6E). In addition, Pak1, which indicates Cdc42 activity and an upstream mediator of CK1α, lost colocalization with NFAT in *Fz8*$^{-/-}$ H2B-GFP^{hi} LRC (Figure S7E). These results suggest that Fz8-mediated noncanonical Wnt signaling blocks NFAT nuclear translocation via the Cdc42-Pak1-CK1α complex. Whether this releasing of NFAT from the Cdc42-Pak1-CK1α complex is triggered by $Ca2^{+}$-induced signal is not clear at this point (see Discussion).

To confirm whether Fmi-Fz8-mediated noncanonical Wnt signaling regulates NFAT nuclear translocation, we observed in quiescent $Fmi^{+}Fz8^{+}$ HSCs that NFAT was mainly localized in the cytoplasm (Figure 6F, upper panel). In contrast, in active $Fmi^{-}Fz8^{-}$HSCs, NFAT was accumulated in the nucleus (Figure 6F, lower panel). Only 4.3% of quiescent HSCs exhibited nuclear localized NFAT, versus 87.7% of active HSCs (Figure 6G). This observation indicates a correlation between cytoplasmic versus nuclear localization of NFAT and the quiescent versus active state of HSCs. When either Fmi or Fz8 was knocked down, more than 80% of LSK cells showed nuclear accumulation of NFAT (Figures 6H and 6I). In addition, Fmi knockdown in OP9 cells induced NFAT nuclear translocation in LSKs cocultured in OP9, suggesting that homophilic interaction of Fmi in adjacent cells regulates NFAT nuclear translocation (Figure S2E).

We examined whether noncanonical Wnts, via Fz8, regulate NFAT cellular localization. As Figure 6J shows, noncanonical Wnt ligands suppress Ca^{2+}-NFAT pathway, while canonical Wnt ligands and *Fz8*$^{-/-}$ promote NFAT nuclear translocation (Figures S7F and S7H). These results indicate that noncanonical Wnt inhibits, but canonical Wnts stimulate, NFAT nuclear translocalization.

To further specify the downstream target genes of NFAT, we found an increase of *IFN*γ expression in *Fmi*$^{-/-}$ (4-fold) and *Fz8*$^{-/-}$ LT-HSCs (3-fold), respectively (Figure 6K). This is consistent with the observation that forced expression of a constitutively active (CA) form of NFAT (Monticelli and Rao, 2002) increased *IFN*γ 2-fold in HSCs (Figure 6L). We observed that noncanonical Wnts downregulated, whereas canonical Wnts upregulated, *IFN*γ expression synergistically in *Fz8*$^{-/-}$ LT-HSCs (Figures 6M and 6N). The upregulation of *IFN*γ expression in $Fz8^{-/-}$ HSCs could not be rescued by noncanonical Wnt5a ligand (Figure 6N) but could be rescued by NFAT inhibitor (NFATi) (Figure 6O). All these results support an antagonization between canonical and non-canonical Wnt signaling in regulating downstream *IFN*γ expression via NFAT.

Furthermore, we examined the change in canonical Wnt signaling in responding to noncanonical Wnt regulation. We confirmed that canonical Wnts, loss of Fz8, and loss of Fmi increased nuclear-localized β-cat-pS552, TOP-Gal staining, and Axin2-d2EGFP level in LT-HSCs (Figures 6P and 6Q; Figures S7I and S7L). *Axin2* was upregulated in active HSCs six times more than in quiescent HSCs (Figure 6R). Taken together, these observations support the conclusion that noncanonical Wnt signaling via Fmi-Fz8 antagonizes canonical Wnt signaling.

Because both IFNs and canonical Wnt have been shown to promote cell proliferation (Baldridge et al., 2010; Essers et al., 2009; Reya and Clevers, 2005), we therefore examined the genes involved in maintaining HSC quiescence, such as *p57*, *Pten*, and *Txnip* (Jeong et al., 2009; Zhang et al., 2006; Zou et al., 2011). We showed these genes to be overall down-regulated to varying degrees in Fmi or Fz8 knockdown HSCs (Figure 6S).

Finally, we tested whether NFAT could activate HSCs by forcing expression of CA-NFAT (Figure 6T). Cell-cycle analysis of LSKs expressing CA-NFAT showed a reduction of quiescent HSCs and a substantial increase of cycling HSCs (Figures 6U and 6V), indicating

that nuclear NFAT promotes HSC activation. We confirmed this observation by showing that NFATi could rescue the reduction in the G0-phase HSCs (Figure 6W).

In summary, we have shown that noncanonical Wnt signaling, mediated by Fmi-Fz8, has two functons: (1) blocking Ca^{2+}-induced NFAT nuclear translocalization and thereby suppressing IFNγ expression, and (2) antagonizing canonical Wnt signaling. Both of these functions contribute to maintaining the quiescence of HSCs.

DISCUSSION

Fmi-Fz8-Mediated Noncanonical Wnt Signaling, Predominantly in the N-cad$^+$OB Niche, Is Critical for Maintaining Quiescent LT-HSCs

We found a correlation between the expression of Fmi and Fz8 in quiescent LT-HSCs and their function in maintaining these HSCs. The remaining question was at which niche component did Fmi and Fz8 primarily function. Multiple HSC niche components have been reported to date, including OBs (particularly N-cad$^+$OBs), endothelial cells, Nestin-GFP$^+$ MSC-like cells, bipotential CAR (CXCL12 abundant reticular) cells, and Schwann cells (Calvi et al., 2003; Kiel et al., 2005; Méndez-Ferrer et al., 2010; Omatsu et al., 2010; Sugiyama et al., 2006; Yamazaki et al., 2011; Zhang et al., 2003). The functional role of OBs was previously tested by Col2.3ΔTK-induced ablation of mature OB cells, and this resulted in a much delayed loss of HSCs (Visnjic et al., 2004). Osteoclasts also influenced HSCs by indirectly regulating osteoblasts (Lymperi et al., 2011). In contrast, genetic ablation of Nestin$^+$ MSCs and CAR cells caused a rapid mobilization of 50%–60% of HSCs from BM to spleen. This was consistent with the distribution of 60% of HSCs in the sinusoidal perivascular niche (Kiel et al., 2005). Notably, the lost or mobilized HSCs were initially proliferating (or active) HSCs (Omatsu et al., 2010). These observations suggested that different niche components may form different microenvironments—quiescent versus active niches (Li and Clevers, 2010).

The perivascular-localized Nestin-GFP and CAR cells, together with endothelial cells, most likely form an active niche (Butler et al., 2010). A recent report showed that SCF was produced in perivascular niche. Conditional deletion of *Scf* in endothelial cells and Leptin$^+$ perivascular cells resulted in ~90% reduction of the number of CD150$^+$CD48$^-$LSK cells, but the remaining HSCs still maintained ~30%–50% reconstitution capacity (Ding et al., 2012). This observation suggested that the remaining HSCs most possibly enrich very quiescent HSCs that were not affected by the loss of SCF (required for cell proliferation and survival) and accounted for the remaining 30%–50% reconstitution capacity.

The endosteal-localized N-cad$^+$OBs in TBR form a quiescent niche (Figures 7A and 7B). In this context, Fmi homophilic adhesion mediates “contact inhibition” (Kimura et al., 2006) to maintain the quiescent state of HSCs in the niche. All these observations support the finding that N-cad$^+$OBs maintain a quiescent niche with dominant noncanonical Wnt signaling and simultaneously suppress canonical Wnt signaling in homeostasis (Figure 7B).

Fmi-Fz8-Mediated Noncanonical Wnt Signaling Suppresses Ca^{2+}-NFAT-IFNγ Pathway and Antagonizes Canonical Wnt Signaling, Thereby Preventing HSC from Activation

Recently, noncanonical Wnt signaling was shown to be involved in HSC development (Clements et al., 2011; Heinonen et al., 2011; Louis et al., 2008) and maintenance in vitro culture (Murdoch et al., 2003; Nemeth et al., 2007), but the underlying mechanism was undefined. Here we observed that noncanonical Wnt signaling, mediated by Fmi-Fz8, restricts NFAT nuclear translocation either through controlling intracellular Ca^{2+} level, potentially through inhibition of LTCC, or via Cdc42-Pak1-CK1α pathway in HSCs. The two events are also very possibly linked because it was reported that CK1α activity can be suppressed by Ca^{2+}-dependent PKC (Zemlickova et al., 2004). Further studies are required to address whether LTCC is functionally required and whether Ca^{2+} through PKC regulates CK1α in HSCs. The link between NFAT and IFNγ in HSCs is physiologically significant as IFNγ plays a critical role in the activation of HSCs (Baldridge et al., 2010; Essers et al., 2009). We would like to point out that IFNγ can also be produced by other cells, such as Treg. Taken together, Fmi- and Fz8-mediated noncanonical Wnt signaling maintains quiescence, partially through downregulation of *IFN*γ expression, and partially via antagonizing canonical Wnt signaling (Figure 7C).

Noncanonical and Canonical Wnt Signaling Have Distinguished Roles, Respectively, in Maintenance versus Activation of HSCs

Wnt signaling, particularly the canonical pathway through activation of β-catenin, has been shown across several species to be prominent in regulating stem cell self-renewal in both embryonic and adult stem cells (Blanpain and Fuchs, 2009; Reya et al., 2003; van de Wetering et al., 2002; Ying et al., 2008). The role of canonical Wnt signaling in HSC maintenance, though, is debatable. For example, forced expression of Dkk1 in osteoblasts suppressed canonical Wnt signaling in HSCs, accompanied by a decrease in quiescent HSCs (Fleming et al., 2008). However, other studies showed that Dkk1-transgenic mice had a defect in trabecular bone (TB) formation (Guo et al., 2010; Li et al., 2006), which is consistent with the observation that absence of β-catenin in osteoblasts led to a defect in TB formation and a subsequent decrease of quiescent HSCs (Nemeth et al., 2009). It is interesting that forced expression of Wif1 in osteoblasts led to a reduction of quiescent HSCs but did not alter bone architecture (Schaniel et al., 2011). This can be explained by the role of Wif1 in inhibiting noncanonical Wnt signaling (Hsieh et al., 1999), and thus increasing canonical Wnt signaling in HSCs (as evidenced by increased Wnt3a).

The association of noncanonical Wnt signaling with N-cad^{+}OBs provides an insight to reconciling previous contradictory observations. For example, Fmi, as an atypical cadherin family molecule, mediates a homophilic interaction between N-cad^{+}OBs and HSCs and provides a redundant role as that of N-cadherin in mediating HSC-niche interaction (Figure 7C). This may account for the subtle phenotype seen in the N-cad conditional knockout model (Kiel et al., 2008).

N-cad^{+}OBs may not simply play a passive role in maintaining quiescent HSCs, as they have been implicated to facilitate HSC expansion in response to irradiation-induced BM damage (Dom-inici et al., 2009). Another report showed the correlation between the number of

HSCs and N-cad^{+}OBs, but not mature OBs (Lymperi et al., 2008). Consistent with this observation, we found that, in response to 5FU-induced BM damage, noncanonical Wnt signaling in N-cad^{+}OBs was attenuated and canonical Wnt signaling was enhanced along with activation of HSCs (Figures 7D and 7E). Our observation provides evidence to distinguish the respective roles of noncanonical and canonical Wnt signaling in maintenance versus activation and expansion of HSCs.

EXPERIMENTAL PROCEDURES

Animals

The transgenic mice used were *Flamingo*$^{-/-}$, *Frizzled8*$^{-/-}$, TRE-mCMV-H2B-GFP, Tal1-tTA, Nestin-GFP, Col2.3-GFP, CD31-GFP, TOP-GAL, and Axin2-d2EGFP. All mice used in this study were housed in the animal facility at the Stowers Institute for Medical Research (SIMR) and handled according to SIMR and National Institutes of Health (NIH) guidelines. All procedures were approved by the Institutional Animal Care and Use Committee (IACUC) of SIMR.

Flow Cytometry

For phenotype analysis, hematopoietic cells were harvested from BM (femur and tibia), spleen, and peripheral blood and lysed. TB and CB were separated according to a previous report (Grassinger et al., 2010). Cell sorting and analysis were performed using a MoFlo (Dako), InFlux Cell Sorter (BD Biosciences), and/or CyAn ADP (Dako). Data analysis was performed using FlowJo software.

Calcium Level Assay

BM cells were incubated in PBS/2% fetal bovine serum (FBS) containing Fluo-3 (Molecular Probes) according to the manufacturer's instructions. Ionomycin (Sigma) was used as a positive control to measure intracellular Ca^{2+} level in LT-HSCs.

Mitochondrial Activity Assay

BM cells were incubated in PBS/2% FBS containing Mitotracker Green FM (Molecular Probes) according to the manufacturer's instructions. The Mito-tracker signal was measured by fluorescein isothiocyanate (FITC) channel in flow cytometry.

Transplantation

Two hundred sorted LSK cells and 2×10^5 rescue BM cells were transplanted for Flamingo and Frizzled8 knockout model. Propidium iode staining was conducted to determine viability of sorted LSK. Fifty percent of cells were alive, which means sorted 200 LSK contained 100 live cells. The mice were analyzed at indicated times posttransplantation.

Repopulation Assay

Sixteen weeks posttransplantation, peripheral blood was collected from submandibular vein. The hematopoietic repopulation was measured from donor-derived blood cells (CD45.2).

RNA Sequencing

The RNA sequencing library was prepared from approximately 200 ng RNA and sequencing on an Illumina HiSeq 2000. The samples were CD31-GFP$^+$ (VEGFR2$^+$CD45$^-$Ter119$^-$) cells, Nestin-GFP$^+$ (CD45$^-$CD31$^-$Ter119$^-$) cells, N-cad$^+$OBs (CD45$^-$CD31$^-$Ter119$^-$), and mature OBs Col2.3-GFP$^+$ (CD45$^-$CD31$^-$Ter119$^-$) for each sample using Illumina TruSeq RNA Sample Prep Kit (catalog number FC-122-1001).

Immunostaining

Paraffin sections of bone were deparaffinized at 60°C for 20 min. Then, the sections were treated with 100% Xylen for 5 min twice, 100% ethanol for 5 min, 95% ethanol for 5 min, 70% ethanol for 5 min, water rinse for 1 min, followed by antigen retrieval with citrate buffer at 90°C for 10 min. Blocking was conducted with Universal Blocking Reagent (BioGenex). For immunostaining of sorted cells, cells were sorted on to lysine-coated slides and fixed with chilled methanol for 10 min followed by blocking and staining with primary antibody. For high-resolution 3D images, the Z-stack images from LSM 510 VIS Confocal Microscopy (Zeiss) were analyzed with Imaris software (Bitplane).

Statistics

Statistics were analyzed with Student’s t test. The results were shown with SD. For additional information, see the Extended Experimental Procedures in the Supplemental Information.

Supplementary Material

Refer to Web version on PubMed Central for supplementary material.

Acknowledgments

We thank A. Paulson and H. Li for RNA-sequencing analysis, and Dr. H. Nakauchi for training in sorted HSC immunostaining. We appreciate Drs. G. Enikolopov, D. Rowe, V. Bautch, E. Fuchs, F. Costantini, and T. Xie for providing these mouse lines respectively: Nestin-GFP, Col2.3-GFP, CD31-ESCs, TOP-GAL, Axin2-d2EGFP, and pSicoR-EF1α. We are grateful to J. Perry and other Li lab members for scientific discussion and critical reading of the manuscript; to M. Hembree, K. Westpfahl, D. Dukes, and B. Lewis for technical support; and to K. Tannen for manuscript editing and proofreading. We thank Y. Takahashi, J. Zhang, X. He, and K. Li for the art and graphic work. This work was funded by SIMR. X.-b. Z. is supported by NIH, National Institute of General Medical Science (Grant GM087376). A.V. is the recipient of an overseas research associateship from the Department of Biotechnology, Government of India. R.S. is a PhD student registered with the Open University.

References

Akashi K, He X, Chen J, Iwasaki H, Niu C, Steenhard B, Zhang J, Haug J, Li L. Transcriptional accessibility for genes of multiple tissues and hematopoietic lineages is hierarchically controlled during early hematopoiesis. Blood. 2003; 101:383–389. [PubMed: 12393558]

Arai F, Hirao A, Ohmura M, Sato H, Matsuoka S, Takubo K, Ito K, Koh GY, Suda T. Tie2/angiopoietin-1 signaling regulates hematopoietic stem cell quiescence in the bone marrow niche. Cell. 2004; 118:149–161. [PubMed: 15260986]

Baldridge MT, King KY, Boles NC, Weksberg DC, Goodell MA. Quiescent haematopoietic stem cells are activated by IFN-gamma in response to chronic infection. Nature. 2010; 465:793–797. [PubMed: 20535209]

Blanpain C, Fuchs E. Epidermal homeostasis: a balancing act of stem cells in the skin. Nat Rev Mol Cell Biol. 2009; 10:207–217. [PubMed: 19209183]

Butler JM, Nolan DJ, Vertes EL, Varnum-Finney B, Kobayashi H, Hooper AT, Seandel M, Shido K, White IA, Kobayashi M, et al. Endothelial cells are essential for the self-renewal and repopulation of Notch-dependent hematopoietic stem cells. Cell Stem Cell. 2010; 6:251–264. [PubMed: 20207228]

Calvi LM, Adams GB, Weibrecht KW, Weber JM, Olson DP, Knight MC, Martin RP, Schipani E, Divieti P, Bringhurst FR, et al. Osteoblastic cells regulate the haematopoietic stem cell niche. Nature. 2003; 425:841–846. [PubMed: 14574413]

Challen GA, Goodell MA. Promiscuous expression of H2B-GFP transgene in hematopoietic stem cells. PLoS ONE. 2008; 3:e2357. [PubMed: 18523660]

Clements WK, Kim AD, Ong KG, Moore JC, Lawson ND, Traver D. A somitic Wnt16/Notch pathway specifies haematopoietic stem cells. Nature. 2011; 474:220–224. [PubMed: 21654806]

Dejmek J, Säfholm A, Kamp Nielsen C, Andersson T, Leandersson K. Wnt-5a/Ca2+-induced NFAT activity is counteracted by Wnt-5a/Yes-Cdc42-casein kinase 1alpha signaling in human mammary epithelial cells. Mol Cell Biol. 2006; 26:6024–6036. [PubMed: 16880514]

Devenport D, Fuchs E. Planar polarization in embryonic epidermis orchestrates global asymmetric morphogenesis of hair follicles. Nat Cell Biol. 2008; 10:1257–1268. [PubMed: 18849982]

Ding L, Saunders TL, Enikolopov G, Morrison SJ. Endothelial and perivascular cells maintain haematopoietic stem cells. Nature. 2012; 481:457–462. [PubMed: 22281595]

Dominici M, Rasini V, Bussolari R, Chen X, Hofmann TJ, Spano C, Bernabei D, Veronesi E, Bertoni F, Paolucci P, et al. Restoration and reversible expansion of the osteoblastic hematopoietic stem cell niche after marrow radioablation. Blood. 2009; 114:2333–2343. [PubMed: 19433859]

Essers MA, Offner S, Blanco-Bose WE, Waibler Z, Kalinke U, Duchosal MA, Trumpp A. IFNalpha activates dormant haematopoietic stem cells in vivo. Nature. 2009; 458:904–908. [PubMed: 19212321]

Fleming HE, Janzen V, Lo Celso C, Guo J, Leahy KM, Kronenberg HM, Scadden DT. Wnt signaling in the niche enforces hematopoietic stem cell quiescence and is necessary to preserve self-renewal in vivo. Cell Stem Cell. 2008; 2:274–283. [PubMed: 18371452]

Fujisaki J, Wu J, Carlson AL, Silberstein L, Putheti P, Larocca R, Gao W, Saito TI, Lo Celso C, Tsuyuzaki H, et al. In vivo imaging of Treg cells providing immune privilege to the haematopoietic stem-cell niche. Nature. 2011; 474:216–219. [PubMed: 21654805]

Grassinger J, Haylock DN, Williams B, Olsen GH, Nilsson SK. Phenotypically identical hemopoietic stem cells isolated from different regions of bone marrow have different biologic potential. Blood. 2010; 116:3185–3196. [PubMed: 20631378]

Gregory MA, Phang TL, Neviani P, Alvarez-Calderon F, Eide CA, O'Hare T, Zaberezhnyy V, Williams RT, Druker BJ, Perrotti D, Degregori J. Wnt/Ca2+/NFAT signaling maintains survival of Ph+ leukemia cells upon inhibition of Bcr-Abl. Cancer Cell. 2010; 18:74–87. [PubMed: 20609354]

Guo J, Liu M, Yang D, Bouxsein ML, Saito H, Galvin RJ, Kuhstoss SA, Thomas CC, Schipani E, Baron R, et al. Suppression of Wnt signaling by Dkk1 attenuates PTH-mediated stromal cell response and new bone formation. Cell Metab. 2010; 11:161–171. [PubMed: 20142103]

Halbleib JM, Nelson WJ. Cadherins in development: cell adhesion, sorting, and tissue morphogenesis. Genes Dev. 2006; 20:3199–3214. [PubMed: 17158740]

Haug JS, He XC, Grindley JC, Wunderlich JP, Gaudenz K, Ross JT, Paulson A, Wagner KP, Xie Y, Zhu R, et al. N-cadherin expression level distinguishes reserved versus primed states of hematopoietic stem cells. Cell Stem Cell. 2008; 2:367–379. [PubMed: 18397756]

He XC, Yin T, Grindley JC, Tian Q, Sato T, Tao WA, Dirisina R, Porter-Westpfahl KS, Hembree M, Johnson T, et al. PTEN-deficient intestinal stem cells initiate intestinal polyposis. Nat Genet. 2007; 39:189–198. [PubMed: 17237784]

Heinonen KM, Vanegas JR, Lew D, Krosl J, Perreault C. Wnt4 enhances murine hematopoietic progenitor cell expansion through a planar cell polarity-like pathway. PLoS ONE. 2011; 6:e19279. [PubMed: 21541287]

Hsieh JC, Kodjabachian L, Rebbert ML, Rattner A, Smallwood PM, Samos CH, Nusse R, Dawid IB, Nathans J. A new secreted protein that binds to Wnt proteins and inhibits their activities. Nature. 1999; 398:431–436. [PubMed: 10201374]

Huang T, Xie Z, Wang J, Li M, Jing N, Li L. Nuclear factor of activated T cells (NFAT) proteins repress canonical Wnt signaling via its interaction with Dishevelled (Dvl) protein and participate in regulating neural progenitor cell proliferation and differentiation. J Biol Chem. 2011; 286:37399–37405. [PubMed: 21880741]

Jeong M, Piao ZH, Kim MS, Lee SH, Yun S, Sun HN, Yoon SR, Chung JW, Kim TD, Jeon JH, et al. Thioredoxin-interacting protein regulates hematopoietic stem cell quiescence and mobilization under stress conditions. J Immunol. 2009; 183:2495–2505. [PubMed: 19625652]

Kalajzic I, Kalajzic Z, Kaliterna M, Gronowicz G, Clark SH, Lichtler AC, Rowe D. Use of type I collagen green fluorescent protein trans-genes to identify subpopulations of cells at different stages of the osteoblast lineage. J Bone Miner Res. 2002; 17:15–25. [PubMed: 11771662]

Kiel MJ, Yilmaz OH, Iwashita T, Yilmaz OH, Terhorst C, Morrison SJ. SLAM family receptors distinguish hematopoietic stem and progenitor cells and reveal endothelial niches for stem cells. Cell. 2005; 121:1109–1121. [PubMed: 15989959]

Kiel MJ, Acar M, Radice GL, Morrison SJ. Hematopoietic stem cells do not depend on N-cadherin to regulate their maintenance. Cell Stem Cell. 2008; 4:170–179. [PubMed: 19119091]

Kimura H, Usui T, Tsubouchi A, Uemura T. Potential dual molecular interaction of the Drosophila 7-pass transmembrane cadherin Flamingo in dendritic morphogenesis. J Cell Sci. 2006; 119:1118–1129. [PubMed: 16507587]

Li J, Sarosi I, Cattley RC, Pretorius J, Asuncion F, Grisanti M, Morony S, Adamu S, Geng Z, Qiu W, et al. Dkk1-mediated inhibition of Wnt signaling in bone results in osteopenia. Bone. 2006; 39:754–766. [PubMed: 16730481]

Li L, Clevers H. Coexistence of quiescent and active adult stem cells in mammals. Science. 2010; 327:542–545. [PubMed: 20110496]

Louis I, Heinonen KM, Chagraoui J, Vainio S, Sauvageau G, Perreault C. The signaling protein Wnt4 enhances thymopoiesis and expands multipotent hematopoietic progenitors through beta-catenin-independent signaling. Immunity. 2008; 29:57–67. [PubMed: 18617424]

Luis TC, Naber BA, Roozen PP, Brugman MH, de Haas EF, Ghazvini M, Fibbe WE, van Dongen JJ, Fodde R, Staal FJ. Canonical wnt signaling regulates hematopoiesis in a dosage-dependent fashion. Cell Stem Cell. 2011; 9:345–356. [PubMed: 21982234]

Lyden D, Hattori K, Dias S, Costa C, Blaikie P, Butros L, Chadburn A, Heissig B, Marks W, Witte L, et al. Impaired recruitment of bone-marrow-derived endothelial and hematopoietic precursor cells blocks tumor angiogenesis and growth. Nat Med. 2001; 7:1194–1201. [PubMed: 11689883]

Lymperi S, Horwood N, Marley S, Gordon MY, Cope AP, Dazzi F. Strontium can increase some osteoblasts without increasing hematopoietic stem cells. Blood. 2008; 111:1173–1181. [PubMed: 17971481]

Lymperi S, Ersek A, Ferraro F, Dazzi F, Horwood NJ. Inhibition of osteoclast function reduces hematopoietic stem cell numbers in vivo. Blood. 2011; 117:1540–1549. [PubMed: 21131587]

Mahmood A, Napoli C, Aldahmash A. In vitro differentiation and maturation of human embryonic stem cell into multipotent cells. Stem Cells Int. 2011; 2011:735420. [PubMed: 21845195]

Malhotra S, Kincade PW. Wnt-related molecules and signaling pathway equilibrium in hematopoiesis. Cell Stem Cell. 2009; 4:27–36. [PubMed: 19128790]

Méndez-Ferrer S, Michurina TV, Ferraro F, Mazloom AR, Macarthur BD, Lira SA, Scadden DT, Ma'ayan A, Enikolopov GN, Frenette PS. Mesenchymal and haematopoietic stem cells form a unique bone marrow niche. Nature. 2010; 466:829–834. [PubMed: 20703299]

Mignone JL, Kukekov V, Chiang AS, Steindler D, Enikolopov G. Neural stem and progenitor cells in nestin-GFP transgenic mice. J Comp Neurol. 2004; 469:311–324. [PubMed: 14730584]

Miharada K, Karlsson G, Rehn M, Rörby E, Siva K, Cammenga J, Karlsson S. Cripto regulates hematopoietic stem cells as a hypoxic-niche-related factor through cell surface receptor GRP78. Cell Stem Cell. 2011; 9:330–344. [PubMed: 21982233]

Mikels AJ, Nusse R. Purified Wnt5a protein activates or inhibits beta-catenin-TCF signaling depending on receptor context. PLoS Biol. 2006; 4:e115. [PubMed: 16602827]

Minta A, Kao JP, Tsien RY. Fluorescent indicators for cytosolic calcium based on rhodamine and fluorescein chromophores. J Biol Chem. 1989; 264:8171–8178. [PubMed: 2498308]

Monticelli S, Rao A. NFAT1 and NFAT2 are positive regulators of IL-4 gene transcription. Eur J Immunol. 2002; 32:2971–2978. [PubMed: 12355451]

Moon RT, Campbell RM, Christian JL, McGrew LL, Shih J, Fraser S. Xwnt-5A: a maternal Wnt that affects morphogenetic movements after overexpression in embryos of Xenopus laevis. Development. 1993; 119:97–111. [PubMed: 8275867]

Murdoch B, Chadwick K, Martin M, Shojaei F, Shah KV, Gallacher L, Moon RT, Bhatia M. Wnt-5A augments repopulating capacity and primitive hematopoietic development of human blood stem cells in vivo. Proc Natl Acad Sci USA. 2003; 100:3422–3427. [PubMed: 12626754]

Murphy LL, Hughes CC. Endothelial cells stimulate T cell NFAT nuclear translocation in the presence of cyclosporin A: involvement of the wnt/glycogen synthase kinase-3 beta pathway. J Immunol. 2002; 169:3717–3725. [PubMed: 12244165]

Nakano T, Kodama H, Honjo T. Generation of lymphohematopoietic cells from embryonic stem cells in culture. Science. 1994; 265:1098–1101. [PubMed: 8066449]

Nemeth MJ, Topol L, Anderson SM, Yang Y, Bodine DM. Wnt5a inhibits canonical Wnt signaling in hematopoietic stem cells and enhances repopulation. Proc Natl Acad Sci USA. 2007; 104:15436–15441. [PubMed: 17881570]

Nemeth MJ, Mak KK, Yang Y, Bodine DM. beta-Catenin expression in the bone marrow microenvironment is required for long-term maintenance of primitive hematopoietic cells. Stem Cells. 2009; 27:1109–1119. [PubMed: 19415781]

Omatsu Y, Sugiyama T, Kohara H, Kondoh G, Fujii N, Kohno K, Nagasawa T. The essential functions of adipo-osteogenic progenitors as the hematopoietic stem and progenitor cell niche. Immunity. 2010; 33:387–399. [PubMed: 20850355]

Panáková D, Werdich AA, Macrae CA. Wnt11 patterns a myocardial electrical gradient through regulation of the L-type Ca(2+) channel. Nature. 2010; 466:874–878. [PubMed: 20657579]

Radtke F, Clevers H. Self-renewal and cancer of the gut: two sides of a coin. Science. 2005; 307:1904–1909. [PubMed: 15790842]

Reya T, Clevers H. Wnt signalling in stem cells and cancer. Nature. 2005; 434:843–850. [PubMed: 15829953]

Reya T, Duncan AW, Ailles L, Domen J, Scherer DC, Willert K, Hintz L, Nusse R, Weissman IL. A role for Wnt signalling in self-renewal of haematopoietic stem cells. Nature. 2003; 423:409–414. [PubMed: 12717450]

Saneyoshi T, Kume S, Amasaki Y, Mikoshiba K. The Wnt/calcium pathway activates NF-AT and promotes ventral cell fate in Xenopus embryos. Nature. 2002; 417:295–299. [PubMed: 12015605]

Schaniel C, Sirabella D, Qiu J, Niu X, Lemischka IR, Moore KA. Wnt-inhibitory factor 1 dysregulation of the bone marrow niche exhausts hematopoietic stem cells. Blood. 2011; 118:2420–2429. [PubMed: 21652676]

Sugiyama T, Kohara H, Noda M, Nagasawa T. Maintenance of the hematopoietic stem cell pool by CXCL12-CXCR4 chemokine signaling in bone marrow stromal cell niches. Immunity. 2006; 25:977–988. [PubMed: 17174120]

Trapnell C, Williams BA, Pertea G, Mortazavi A, Kwan G, van Baren MJ, Salzberg SL, Wold BJ, Pachter L. Transcript assembly and quantification by RNA-Seq reveals unannotated transcripts and isoform switching during cell differentiation. Nat Biotechnol. 2010; 28:511–515. [PubMed: 20436464]

Tumbar T, Guasch G, Greco V, Blanpain C, Lowry WE, Rendl M, Fuchs E. Defining the epithelial stem cell niche in skin. Science. 2004; 303:359–363. [PubMed: 14671312]

Usui T, Shima Y, Shimada Y, Hirano S, Burgess RW, Schwarz TL, Takeichi M, Uemura T. Flamingo, a seven-pass transmembrane cadherin, regulates planar cell polarity under the control of Frizzled. Cell. 1999; 98:585–595. [PubMed: 10490098]

van de Wetering M, Sancho E, Verweij C, de Lau W, Oving I, Hurlstone A, van der Horn K, Batlle E, Coudreuse D, Haramis AP, et al. The beta-catenin/TCF-4 complex imposes a crypt progenitor phenotype on colorectal cancer cells. Cell. 2002; 111:241–250. [PubMed: 12408868]

Visnjic D, Kalajzic Z, Rowe DW, Katavic V, Lorenzo J, Aguila HL. Hematopoiesis is severely altered in mice with an induced osteoblast deficiency. Blood. 2004; 103:3258–3264. [PubMed: 14726388]

Wilson A, Laurenti E, Oser G, van der Wath RC, Blanco-Bose W, Jaworski M, Offner S, Dunant CF, Eshkind L, Bockamp E, et al. Hematopoietic stem cells reversibly switch from dormancy to self-renewal during homeostasis and repair. Cell. 2008; 135:1118–1129. [PubMed: 19062086]

Xie Y, Yin T, Wiegraebe W, He XC, Miller D, Stark D, Perko K, Alexander R, Schwartz J, Grindley JC, et al. Detection of functional haematopoietic stem cell niche using real-time imaging. Nature. 2009; 457:97–101. [PubMed: 19052548]

Yamazaki S, Ema H, Karlsson G, Yamaguchi T, Miyoshi H, Shioda S, Taketo MM, Karlsson S, Iwama A, Nakauchi H. Nonmyelinating Schwann cells maintain hematopoietic stem cell hibernation in the bone marrow niche. Cell. 2011; 147:1146–1158. [PubMed: 22118468]

Yang L, Bryder D, Adolfsson J, Nygren J, Månsson R, Sigvardsson M, Jacobsen SE. Identification of Lin(−)Sca1(+)kit(+)CD34(+)Flt3-short-term hematopoietic stem cells capable of rapidly reconstituting and rescuing myeloablated transplant recipients. Blood. 2005; 105:2717–2723. [PubMed: 15572596]

Ying QL, Wray J, Nichols J, Batlle-Morera L, Doble B, Woodgett J, Cohen P, Smith A. The ground state of embryonic stem cell self-renewal. Nature. 2008; 453:519–523. [PubMed: 18497825]

Zemlickova E, Johannes FJ, Aitken A, Dubois T. Association of CPI-17 with protein kinase C and casein kinase I. Biochem Biophys Res Commun. 2004; 316:39–47. [PubMed: 15003508]

Zhang J, Niu C, Ye L, Huang H, He X, Tong WG, Ross J, Haug J, Johnson T, Feng JQ, et al. Identification of the haematopoietic stem cell niche and control of the niche size. Nature. 2003; 425:836–841. [PubMed: 14574412]

Zhang J, Grindley JC, Yin T, Jayasinghe S, He XC, Ross JT, Haug JS, Rupp D, Porter-Westpfahl KS, Wiedemann LM, et al. PTEN maintains haematopoietic stem cells and acts in lineage choice and leukaemia prevention. Nature. 2006; 441:518–522. [PubMed: 16633340]

Zhou L, Bar I, Achouri Y, Campbell K, De Backer O, Hebert JM, Jones K, Kessaris N, de Rouvroit CL, O'Leary D, et al. Early forebrain wiring: genetic dissection using conditional Celsr3 mutant mice. Science. 2008; 320:946–949. [PubMed: 18487195]

Zou P, Yoshihara H, Hosokawa K, Tai I, Shinmyozu K, Tsukahara F, Maru Y, Nakayama K, Nakayama KI, Suda T. p57(Kip2) and p27(Kip1) cooperate to maintain hematopoietic stem cell quiescence through interactions with Hsc70. Cell Stem Cell. 2011; 9:247–261. [PubMed: 21885020]

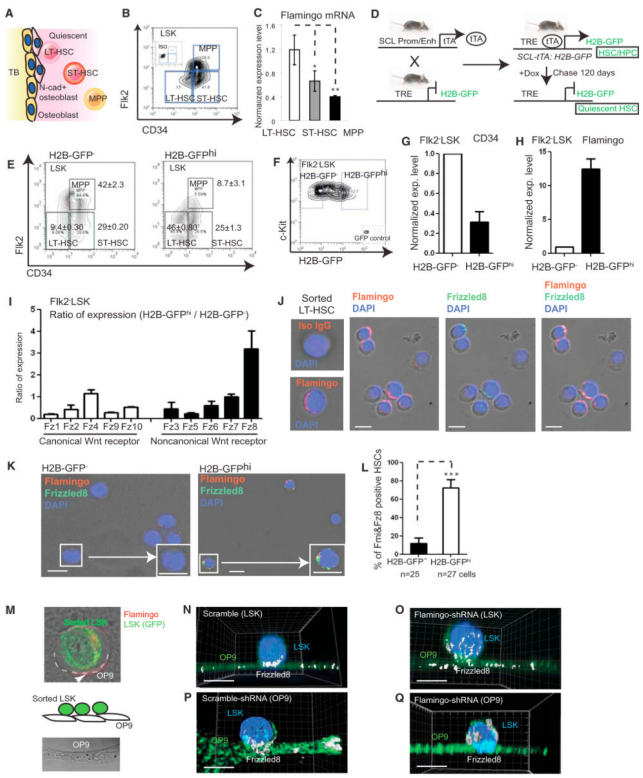

Figure 1. Fmi Regulates Noncanonical Wnt Receptor Fz8 Distribution in Quiescent LT-HSCs

(A and B) Scheme and gating of LT-HSCs, ST-HSCs, and MPPs.

(C) qRT-PCR of *Fmi* in sorted LT-HSCs, ST-HSCs, and MPPs in a setting of triplicates (hereinafter).

(D) Scl-tTA-induced H2B-GFP label retention in HSCs.

(E) Percentage of LT-HSCs, ST-HSCs, and MPPs in H2B-GFP^{-}LSK and H2B-GFP^{hi}LSK.

(F) Gating H2B-GFP HSCs.

(G–I) qRT-PCR of *CD34* (G), *Fmi* (H), and *Fzs* (I).

(J and K) Immunostaining Fmi and Fz8 in sorted LT-HSCs (J) and H2B-GFP HSCs (K).

(L) Percentage of Fmi and Fz8 expressed in sorted H2B-GFP HSCs.

(M) Immunostaining Fmi in sorted GFP^{+}LSK cells and OP9 osteoprogenitors.

(N–Q) 3D images of Fz8 in LSK on OP9. Scale bar, 5 μM. *p < 0.05. **p < 0.01. ***p < 0.001. Values shown as mean ± SD.

See Figure S1.

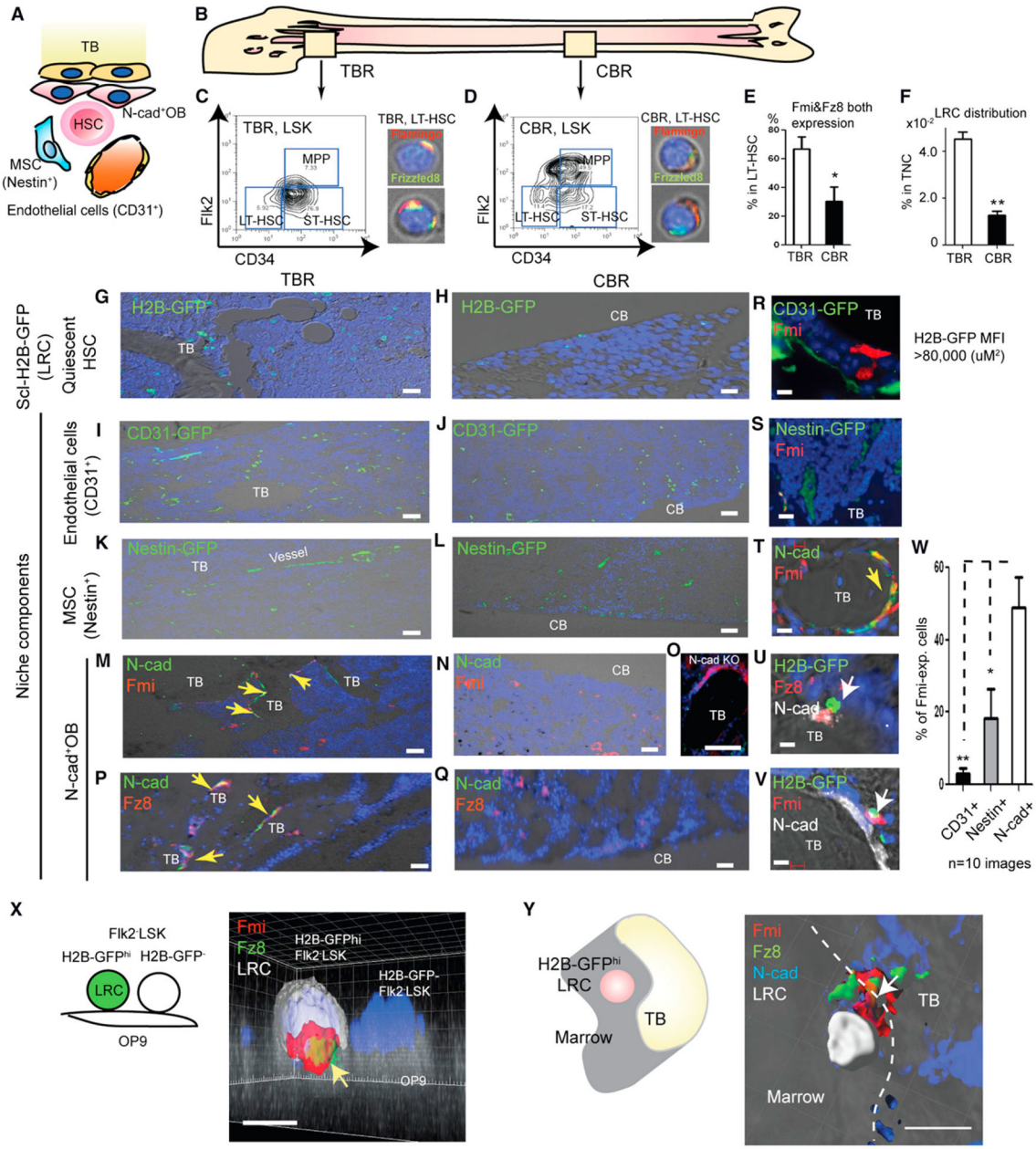

Figure 2. Fmi and Fz8 Colocalize at the Interface between Quiescent LT-HSCs and N-cad^{+}OBs in TBR

(A) HSC and N-cad^{+}OB, Nestin^{+}-MSC, and endothelial cells (CD31^{+}).

(B) The sagittal section of Femur.

(C and D) Sorted LT-HSCs from TBR (C) and CBR (D) and immunostaining Fmi and Fz8.

(E and F) Percentage of LT-HSCs and H2B-GFP^{hi} label-retaining cells (LRCs) in total nuclear cell (TNC) expressing both Fmi and Fz8.

(G–V) Location of quiescent HSCs (G and H) or niche components: CD31-GFP (I and J), Nestin-GFP (K and L), N-cad^{+}OB (M–Q). Scale bar, 20 μM. (R–V) Scale bar, 5 μM.

(W) Percentage of niche expressing Fmi.

(X) 3D image of sorted HSC on OP9. Colocalization of Fmi and Fz8 (yellow arrow) between H2b-GFP^{hi} HSC and OP9 osteoprogenitor.
(Y) 3D images of LRC (white, MFI = 122,009 uM^2). Colocalization of Fmi and Fz8 (white arrow) at the interface between N-cad$^+$ OB and H2b-GFP^{hi} HSC. *p < 0.05. **p < 0.01. ***p < 0.001. Values shown as mean ± SD.
See Figure S2.

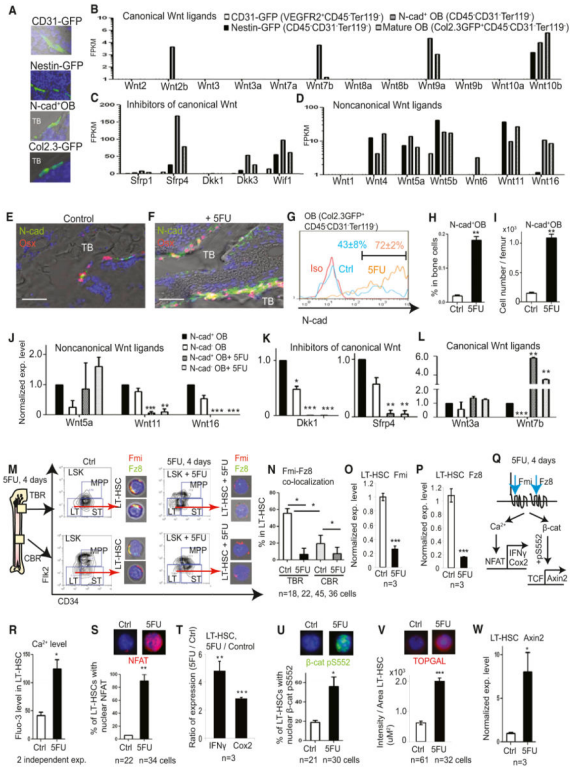

Figure 3. N-cad^{+}OBs Maintain Dominant Noncanonical Wnt Signaling, which Is Attenuated Under Stress

(A) BM section with CD31-GFP, Nestin-GFP, N-cad^{+}OB, and Col2.3-GFP, respectively (shown in green).

(B–D) RNA sequencing analysis of sorted niche components for Wnt signaling related genes.

See Table S1 for FPKM value.

(E and F) Immunostaining TBR. Scale bar, 20 μM.

(G) Flow cytometry analysis of N-cad^{+} OBs percentage in homeostatic (blue) and 5FU-treated (red) conditions.

(H and I) Frequency and number of N-cad^{+}OBs in bone cells.

(J–L) qRT-PCR analysis of Wnt-related genes.

(M and N) Fmi and Fz8 staining in LT-HSCs.

(O and P) Measurement of *Fmi* and *Fz8* levels.

(Q) Noncanonical Wnt signaling.

(R) Ca^{2+} level in LT-HSCs post-5FU.

(S–W) Protein and mRNA levels of LT-HSCs post-5FU: NFAT (S), NFAT targets (T), β-catenin-pS552 (U), TOP-GAL (V), and *Axin2* (W). *p < 0.05. **p < 0.01. ***p < 0.001. Values shown as mean ± SD.

See Figures S3 and S4.

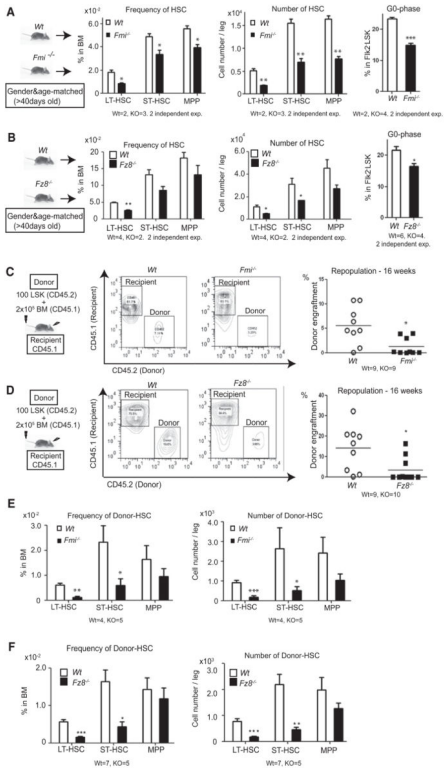

Figure 4. Fmi and Fz8 Are Required for the Function of LT-HSCs In Vivo

(A and B) Analyses of conventional Fmi (A) or Fz8 (B) knockout mice. Frequency, number, and cell cycle (G0 phase) of HSCs.

(C and D) Repopulation analysis of mice receiving transplanted donor cells: 100 LSK (CD45.2) + 2×10^5 BM (CD45.1). Recipients were lethally radiated (CD45.1). Repopulation analysis 16 weeks after injection.

(E and F) Frequency and number of donor HSCs 17 weeks posttransplantation. *$p < 0.05$. **$p < 0.01$. ***$p < 0.001$. Values shown as mean ± SD.

See Figures S5 and S6.

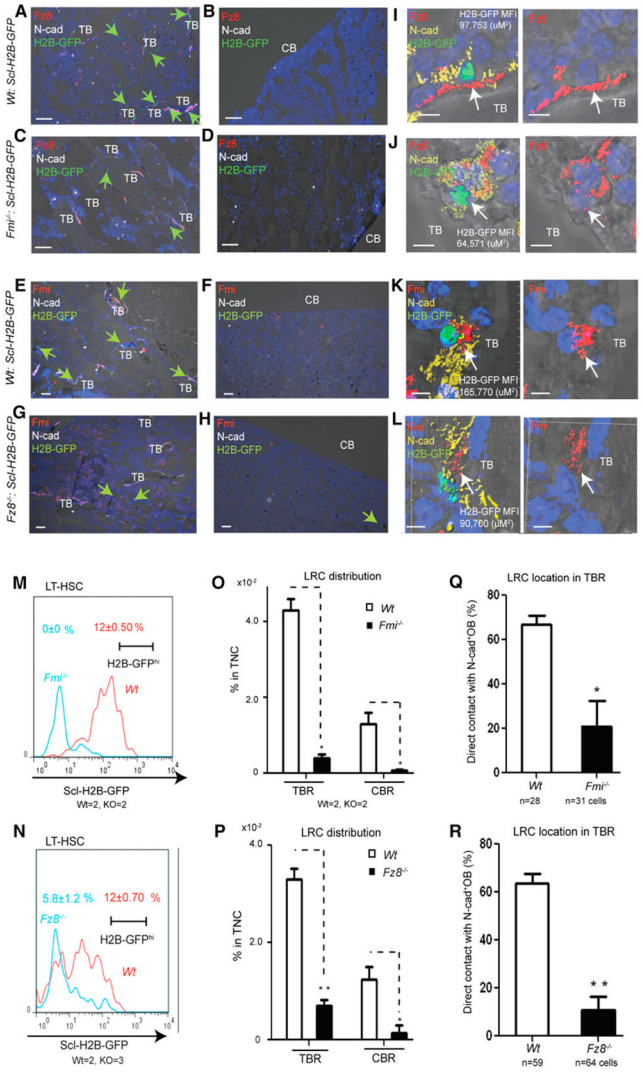

Figure 5. Fmi and Fz8 Maintain Quiescence of LT-HSCs In Vivo

(A–H) Immunostaining of Fz8 (A–D) Fmi (E–H), N-cad, and H2B-GFP^{hi} LRC in TBR and CBR from *Wt: Scl-H2B-GFP*, *Fmi$^{-/-}$: Scl-H2B-GFP*, and *Fz8$^{-/-}$: Scl-H2B-GFP*. Scale bar, 20 μM.

(I–L) 3D image of protein localization (white arrow). Scale bar, 5 μM.

(M and N) Flow cytometry analysis of H2B-GFP intensity in LT-HSCs.

(O and P) LRC distribution in TBR and CBR.

(Q and R) Frequency of LRC directly contacting N-cad^{+}OBs in TBR. *p < 0.05. **p < 0.01. ***p < 0.001. Values shown as mean ± SD.

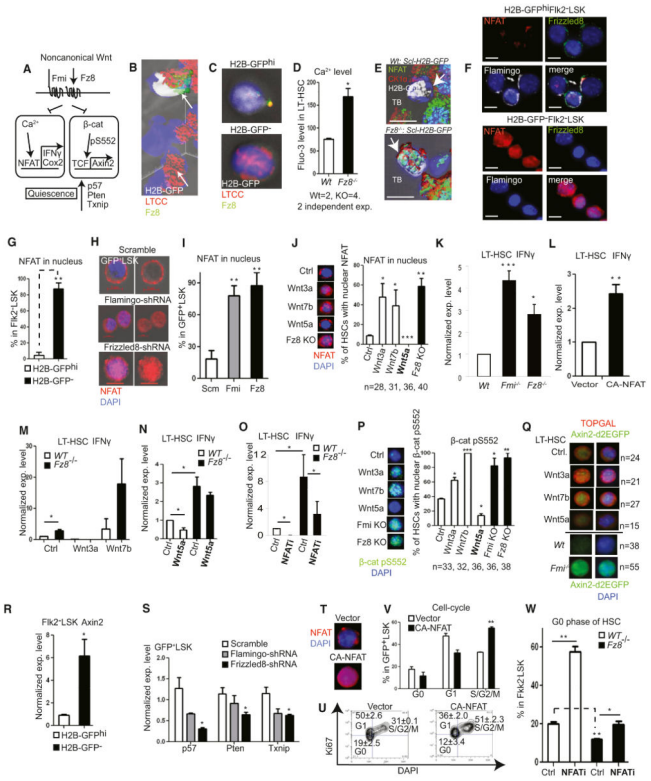

Figure 6. Noncanonical Wnt Signaling Mediated by Fz8 Suppresses NFAT-Induced IFNγ Expression and Antagonizes Canonical Wnt Signaling

(A) Ca^{2+}-NFAT and β-catenin pathways.

(B and C) LTCC and Fz8 localization in vivo (B) and sorted HSCs (C).

(D) Ca^{2+} level in LT-HSCs in *Wt* and *Fz8*$^{-/-}$ mice.

(E) NFAT and CK1α localization in LRC of *Wt* and *Fz8*$^{-/-}$ mice.

(F and G) Fmi, Fz8, and NFAT staining in sorted HSCs. Scale bar, 5 μM.

(H and I) LSK from Fmi-shRNA Fz8-shRNA transfected mice were stained with NFAT.

(J) NFAT immunostaining of LT-HSCs.

(K–O) *IFNγ* expression in LT-HSCs.

(P and Q) β-catenin-pS552 staining (P) and TOP-GAL and Axin2-d2EGFP (Q) staining in LT-HSCs.

(R) *Axin2* expression in HSCs.

(S) Expression of quiescence-related genes.

(T) Immunostaining of NFAT.

(U and V) Cell-cycle analysis of GFP^{+}LSK cells.

(W) Percentage of quiescent HSCs. *p < 0.05. **p < 0.01. ***p < 0.001. Values shown as mean ± SD.

See Figure S7.

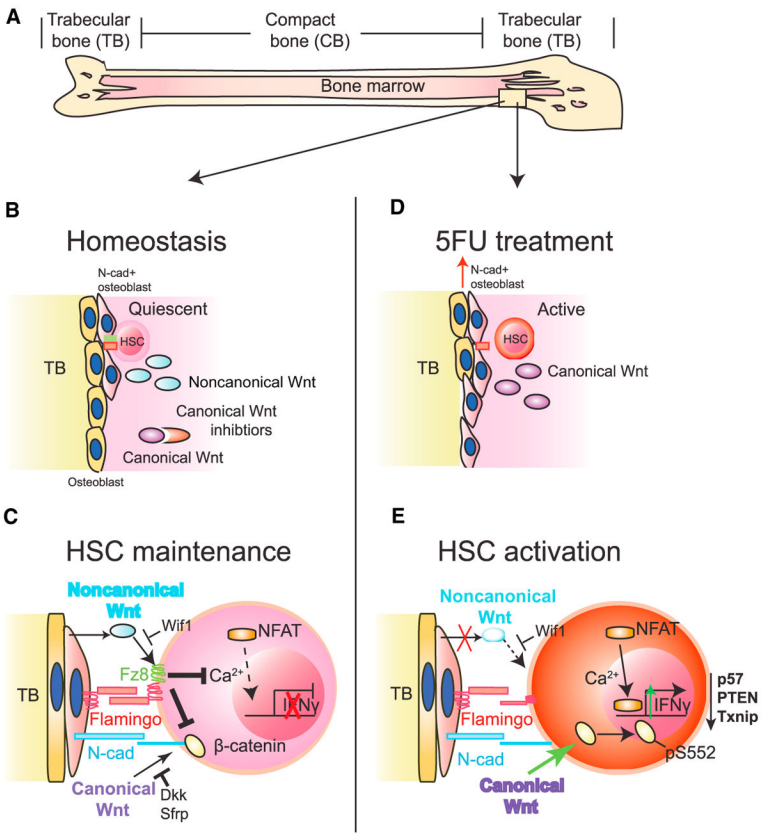

Figure 7. Noncanonical Wnt Signaling Maintains Quiescent LT-HSCs through Fmi and Fz8 Interaction in the Niche

(A) The sagittal section of Femur.

(B) N-cad+ OBs maintain a predominant non-canonical Wnt signaling that maintain quiescent HSCs during homeostasis.

(C) Fz8 suppresses Ca^{2+}-NFAT nuclear translocation and NFAT-dependent *IFN*γ expression.

(D) Upregulation of canonical Wnt signaling and HSC activation in response to 5FU treatment.

(E) Decrease in Fmi-Fz8-mediated noncanonical Wnt signaling resulted from NFAT-induced *IFN*γ expression and an increase in canonical Wnt signaling, thus together promoting HSC activation.